Journal of Systems Engineering and Electronics
Vol. 35, No. 4, August 2024, pp.815 – 828

High performance receiving and processing technology in satellite beam hopping communication

ZHAI Shenghua[1,2], HUI Tengfei[1,2,*], GONG Xianfeng[1,2], ZHANG Zehui[3], GAO Xiaozheng[4], and YANG Kai[4]

1. School of Communication Engineering, Xi'Dian University, Xian 710126, China;
2. CAST (China Academy of Space Technology)-Xi'an Institute of Space Radio Technology, Xi'an 710010, China;
3. School of Cyberspace Science and Technology, Beijing Institute of Technology, Beijing 100081, China;
4. School of Information and Electronics, Beijing Institute of Technology, Beijing 100081, China

Abstract: Beam-hopping technology has become one of the major research hotspots for satellite communication in order to enhance their communication capacity and flexibility. However, beam hopping causes the traditional continuous time-division multiplexing signal in the forward downlink to become a burst signal, satellite terminal receivers need to solve multiple key issues such as burst signal rapid synchronization and high-performance reception. Firstly, this paper analyzes the key issues of burst communication for traffic signals in beam hopping systems, and then compares and studies typical carrier synchronization algorithms for burst signals. Secondly, combining the requirements of beam-hopping communication systems for efficient burst and low signal-to-noise ratio reception of downlink signals in forward links, a decoding assisted bidirectional variable parameter iterative carrier synchronization technique is proposed, which introduces the idea of iterative processing into carrier synchronization. Aiming at the technical characteristics of communication signal carrier synchronization, a new technical approach of bidirectional variable parameter iteration is adopted, breaking through the traditional understanding that loop structures cannot adapt to low signal-to-noise ratio burst demodulation. Finally, combining the DVB-S2X standard physical layer frame format used in high throughput satellite communication systems, the research and performance simulation are conducted. The results show that the new technology proposed in this paper can significantly shorten the carrier synchronization time of burst signals, achieve fast synchronization of low signal-to-noise ratio burst signals, and have the unique advantage of flexible and adjustable parameters.

Keywords: beam-hopping, high throughput satellite, high performance, reception processing.

DOI: 10.23919/JSEE.2024.000076

1. Introduction

With the advancement of satellite internet applications, satellite communication technology is progressing towards high throughput satellite (HTS) communication systems. HTS utilizes technologies such as point beam, fugitive beam, and frequency multiplexing to provide several to tens of times more capacity than conventional satellites under the same orbit and spectrum conditions. Beam hopping technology has become one of the major research areas for HTSs to enhance their communication capacity and flexibility.

At the same time, existing forward service communication systems mainly use standard systems such as DVB-S2/S2X, which usually use high-performance compiled codes such as low density parity check (LDPC) code as channel coding. The high-performance LDPC codes further reduce the working threshold of communication demodulation, thus the demodulation of low signal-to-noise ratio (SNR) burst signals becomes the key to the processing of hopping beam service communication.

In digital receivers, the most critical part of demodulation technology is synchronization technology, which requires carrier synchronization and bit timing synchronization to be implemented in the receiver. Digital communication can be divided into continuous communication mode and burst communication mode. The burst communication mode involves a short transmission time signal, where data is transmitted using multiple discontinuous time slots, and a transmission time slot is often referred to as a time slot. Burst communication is more com-

Manuscript received April 14, 2023.
*Corresponding author.
This work was supported by the Key Research and Development Program of Shaanxi (2022ZDLGY05-08), the Application Innovation Program of CASC (China Aerospace Science and Technology Corporation) (6230107001), the Research Project on Civil Aerospace Technology (D040304), the Research Project of CAST (Y23-WYHXJS-07) and the Research Foundation of the Key Laboratory of Spaceborne Information Intelligent Interpretation (2022-ZZKY-JJ-20-01).

plex in terms of demodulation and synchronization as the burst signal is very short and the efficiency of the transmission frame format has to be taken into account. In burst communication, in order to ensure the performance of the receiver, a certain length of leading symbol is usually required to transmit synchronization information. The choice of the leading symbol's length is influenced by several factors. A longer leading symbol makes it easier for the receiver to synchronize, but it also reduces the frame efficiency. On the other hand, a shorter leading symbol makes it more challenging for the receiver to synchronize, but it increases the frame efficiency.

The successful application of hopping beam technology in HTS communication systems requires achieving high frame efficiency and low SNR simultaneously. This means that signal reception needs to be completed with a short leading head and low SNR, while also achieving a bit error rate (BER) level comparable to that of standard systems like DVB-S2/S2X [1]. However, this presents technical challenges such as fast capture of burst signals, high precision bit synchronization of burst signals, and high precision carrier synchronization of burst signals.

2. Burst signal carrier synchronization technology

The hopping beam technology of the HTS system is implemented in the forward link of the system, where several user beams combine to form a beam cluster and share frequency and power resources in a time-sharing manner. In order to ensure that the signal reaches the intended user beam, the satellite performs precise time and space switching and forwarding. Fig. 1 shows a schematic diagram of the forward downlink using the hopping beam technique.

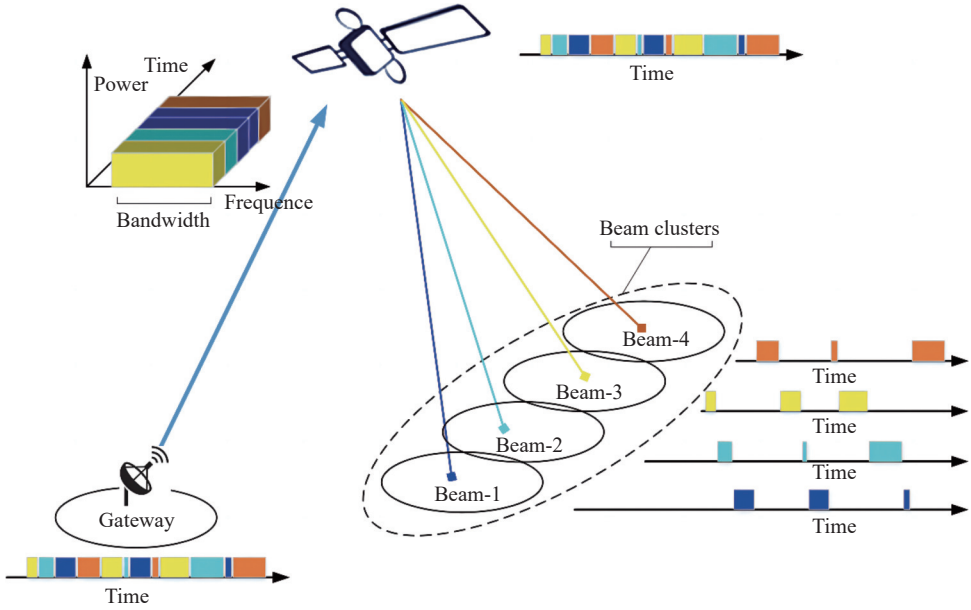

Fig. 1 Schematic diagram of the forward downlink using the hopping beam technique

In Fig. 1, a beam cluster is formed by four user beams, and the signal gateway station plans the communication data flow in time in the form of burst signal packets according to the communication service requirements of each beam, and the four user beams share the downlink frequency and power resources of the satellite in space in a time-sharing manner.

Satellite beam hopping optimizes system capacity and flexibility of use, but as beam hopping causes the traditional continuous time-division multiplexing (TDM) signal in the forward downlink to become a burst TDM signal, ground receivers need to adapt to demodulation in burst mode, placing demands on the ground demodulator for fast synchronization.

Burst signal detection can use time domain detection or frequency domain detection methods. It presents a time domain signal detection algorithm that utilizes multiplexed differential correlation and has been shown to have strong detection capabilities at low SNRs in previous studies [2]. This algorithm has a lead length of 192 symbols and E_S/N_0= 2 dB. The miss detection rate and false detection rate are both lower than 10^{-5}, which provides a viable solution to the burst signal capture problem under low SNR conditions.

Symbol synchronization, also known as code-element synchronization, is widely used based on interpolation filtering [3]. It proposes an energy comparison-based symbol synchronization method in [4]. When the symbol sampling rate is 8, the theoretical normalized timing deviation after synchronization using this algorithm does not

exceed 0.125 code-element cycles. Additionally, increasing the number of code elements for weighted averaging can reduce the applicable threshold of the algorithm. The E_S/N_0 operating threshold can be lower than 0 dB.

In coherent demodulation, in addition to bit synchronization, carrier synchronization is a separate challenge, which consists of frequency synchronization and phase synchronization. These components have specific requirements of the lowest possible SNR and the smallest possible phase error. Carrier synchronization also has performance requirements, including a fast synchronization build-up time and long hold time. For burst channels in satellite communications, carrier synchronization requirements are even more stringent. The carrier synchronization time must not only be fast but also highly reliable.

2.1 Closed-loop carrier synchronization algorithm

Various closed-loop carrier synchronization algorithms are available, with Fig. 2 showing a fine-grained phase recovery algorithm that is commonly used in DVB-S2 receivers [5]. This algorithm is essentially a conventional phase-locked loop (PLL) structure with a process that involves multiplication and discrimination of the input sample signal with two local orthogonal carrier signals. The discriminated result is filtered and demodulated, and then fed to the phase detector to obtain the error signal. This signal is filtered in the loop and controls look-up table to produce the local carrier, which is then multiplied with the input data to form a closed loop. The loop filter is usually in the form of a second or third order to ensure accurate tracking of the input signal phase, frequency, frequency change rate, and other parameters, thereby reducing the system's error performance. The loop bandwidth selection is crucial since it directly affects the algorithm's capture speed and synchronization accuracy, which is a key design trade-off. Additionally, to improve the loop's capture performance, initial frequency and phase estimation are often used. The algorithm has an advantage since, once the initial carrier synchronization is complete, it can automatically track changes in frequency and phase bias, and the parameters are chosen appropriately to ensure high tracking accuracy, thereby resulting in a relatively good receiver BER performance.

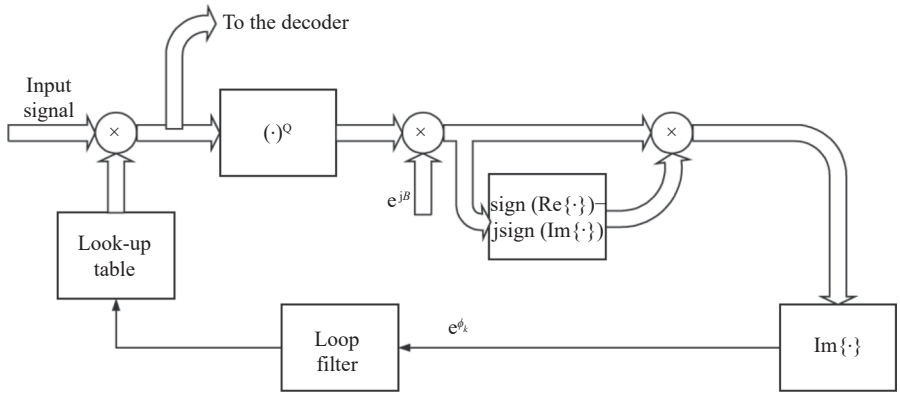

Fig. 2 Carrier synchronization algorithm used in DVB-S2 receivers

To visualize the performance of the algorithm, the simulation parameters are as follows, the modulation signal is a quadrature phase shift keying (QPSK) signal, the initial frequency bias $\Delta f = -50$ kHz, the symbol rate $f_s =$ 3 MHz and the sampling frequency is 24 MHz. Simulation results are shown in Fig. 3 and Fig. 4.

From the simulation results, it can be seen that when the SNR is relatively high, the proposed algorithm can quickly achieve synchronization. However, when the SNR is low, the locking time becomes significantly longer. In low SNR conditions, in order to ensure the accuracy of carrier tracking, a very narrow loop bandwidth parameter is required. However, this can inevitably lead to longer acquisition times, which is a common issue with such closed-loop algorithms. Considering the above reasons, the main challenge for applying such closed-loop carrier synchronization algorithms in burst communication is how to achieve fast capture of signal phase within a relatively short signal duration.

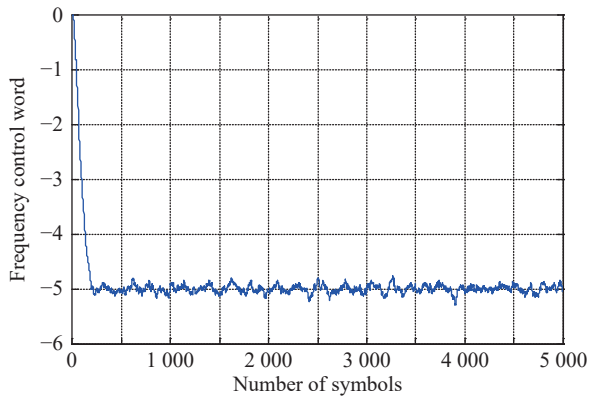

Fig. 3 Algorithm frequency response curve at SNR=10 dB

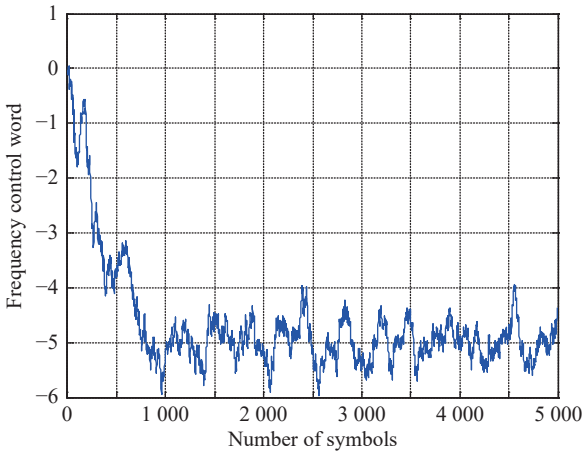

Fig. 4 Algorithm frequency response curve at SNR=4 dB

2.2 Open-loop carrier synchronization algorithm

Commonly used open-loop carrier parameter estimation algorithms include frequency domain estimation algorithms and time domain estimation algorithms. A frequency domain estimation method detects coarse frequency values by searching for peaks and uses spectral line information for accurate estimation in [6]. On the other hand, time-domain estimation algorithms extract frequency bias information from signal autocorrelation values. High estimation accuracy at high SNR can be achieved with the Kay estimation algorithm and its related improvements in the time domain algorithm [7–10]. In the frequency domain algorithms, the Rife algorithm and its related improvements are used by searching for periodogram peaks [11–14].

(i) Mathematical model of open-loop frequency bias estimation algorithm

It is assumed that bit synchronization has been achieved prior to frequency bias estimation and that the point used for estimation is the best sampled point. The received QPSK signal containing the data information and the carrier frequency bias can be expressed as

$$r(k)=\exp(\mathrm{j}(2\pi\Delta f T_s k+\phi_k+\theta))+n(k)=$$
$$A_k\exp(\mathrm{j}(2\pi\Delta f T_s k+\phi_k+\theta+\alpha_k)),\ \ 0\leqslant k\leqslant L-1. \tag{1}$$

The mathematical model of the open-loop frequency bias estimation algorithm can be described as follows. Δf represents the carrier frequency difference, T_s represents the symbol period, and $n(k)\sim \mathrm{N}(0,2\sigma^2)$ represents the additive complex Gaussian noise with equal variances σ^2 for its in-phase and quadrature components. θ represents the predetermined phase difference of the carrier, A_k represents the instantaneous amplitude of the signal, α_k represents the equivalent phase noise, ϕ_k represents the phase value of the data modulation, and $\phi_k\in\{\pm\pi,\pm 3\pi/4\}$.

After the bit synchronization, the modulation information is removed using the known preamble sequence $\boldsymbol{C}(k)$, resulting in a sequence $Z(k)=r(k)\cdot\boldsymbol{C}^*(k)=\mathrm{e}^{\mathrm{j}(2\pi\Delta T_s k+\theta)}+n(k)$ containing only frequency and phase offset information, where * indicates conjugate transposition. The frequency offset estimation algorithm then uses the samples $\{Z(k),1\leqslant k\leqslant L\}$ to estimate the carrier frequency offset.

(ii) Carrier frequency bias estimation algorithm based on periodogram

The fast Fourier transform (FFT) frequency offset estimation algorithm is a typical representative of carrier frequency offset estimation algorithms based on periodograms. The basic idea is to perform demodulation on the input base band sampled signal and then perform an N-point FFT transformation. By searching for the amplitude peak of the transformed data, the frequency deviation is calculated. The value of N determines the estimation accuracy of the frequency deviation, and a specific selection needs to balance the trade-off between computational complexity and accuracy. The structure of the FFT frequency offset estimation algorithm is shown in Fig. 5.

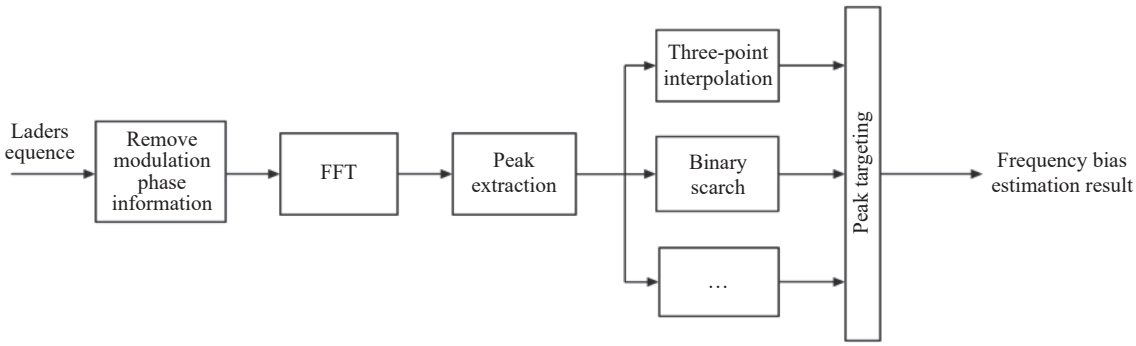

Fig. 5 Structure of the frequency bias estimation algorithm

The N-point discrete Fourier transform (DFT) of the demodulated signal from $Z(k)$ is used to obtain the spectrum:

$$F(n)=\sum_{k=0}^{N-1}Z(k)\mathrm{e}^{-\mathrm{j}\frac{2\pi}{N}kn}=|F(n)|\mathrm{e}^{\mathrm{j}\varphi(n)} \tag{2}$$

where n=0, 1, ⋯, N−1. $n_{\max}$, the value of n that maxi-

mizes the amplitude-frequency characteristic $|F(n)|$ of the DFT is searched. Then, according to the maximum likelihood estimation theory, the maximum likelihood estimation value of the frequency offset f_d can be obtained as

$$\hat{f}_d = \begin{cases} \dfrac{n_{\max}}{4T_aN}, & 0 \leqslant n_{\max} \leqslant \dfrac{N}{2}-1 \\ -\dfrac{N-n_{\max}}{4T_aN}, & \dfrac{N}{2} \leqslant n_{\max} \leqslant N-1 \end{cases}. \tag{3}$$

The spectral spacing of spectral lines for the accuracy of the frequency bias estimate calculated by the N-point FFT is $(MT_aN)^{-1}$. If the peak value of the actual signal spectrum is the same as the peak value spectrum line of the FFT amplitude-frequency characteristic, there is no frequency estimation bias. If they are different, it must appear between two spectral lines, and in practical calculations, the spectral line with the smallest distance to the peak value can be selected as the frequency offset estimation result. Therefore, the maximum estimation error of the FFT frequency offset estimation algorithm is

$$|\Delta\hat{f}_d| = \frac{1}{2}\frac{1}{4T_aN} = \frac{1}{8}\frac{1}{ST_sN}. \tag{4}$$

When high synchronization accuracy is required, the introduced estimation error by the FFT algorithm cannot be tolerated. Therefore, in recent years, a large amount of research has been devoted to reducing the estimation error introduced by the FFT algorithm. There are generally two directions that one is to perform frequency interpolation, and the other is to use some iteration algorithm to obtain the accurate value after the initial estimation. Here, we introduce the most commonly used binary frequency search method.

(iii) Binary frequency search algorithm

To further approach the true value of frequency offset estimation and facilitate carrier synchronization and tracking, a binary search method can be designed to search for the true peak position of the spectrum and improve the accuracy of frequency estimation. The binary search can be performed in the following steps.

Step 1 Initialize the frequency step Δ to be searched for, using the peak position m obtained from the FFT as the initial point, and calculate

$$\begin{cases} |F_1| = \left|\sum\limits_{i=0}^{N-1} Z_i \mathrm{e}^{-\mathrm{j}\frac{2\pi}{N}i(m-\Delta)}\right| \\ |F_2| = \left|\sum\limits_{i=0}^{N-1} Z_i \mathrm{e}^{-\mathrm{j}\frac{2\pi}{N}im}\right| \\ |F_3| = \left|\sum\limits_{i=0}^{N-1} Z_i \mathrm{e}^{-\mathrm{j}\frac{2\pi}{N}i(m+\Delta)}\right| \end{cases}. \tag{5}$$

Step 2 Make $\Delta = \dfrac{\Delta}{2}$. If $|F_1| > |F_3|$, then $m = m - \Delta$, $|F_1| = |F_1|$, $|F_3| = |F_2|$; if $|F_1| < |F_3|$, then $m = m + \Delta$, $|F_1| = |F_2|$, $|F_3| = |F_3|$, $|F_2| = \left|\sum\limits_{i=0}^{N-1} Z_i \mathrm{e}^{-\mathrm{j}\frac{2\pi}{N}im}\right|$.

Step 3 Repeat Step 2 until Δ achieves the required accuracy. At this point, the frequency bias estimate can be obtained as

$$\hat{f}_d = \begin{cases} \dfrac{m}{4T_aN}, & 0 \leqslant m \leqslant \dfrac{N}{2}-1 \\ -\dfrac{N-m}{4T_aN}, & \dfrac{N}{2} \leqslant m \leqslant N-1 \end{cases}. \tag{6}$$

(iv) Carrier phase estimation

With the above steps, the carrier frequency bias estimation is completed. Next, the initial frequency bias is compensated for using the estimation results to obtain the following signal:

$$r'(k) = \left(\mathrm{e}^{\mathrm{j}(2\pi\Delta fT_sk+\phi_k+\theta)} + n(k)\right)\mathrm{e}^{-\mathrm{j}2\pi\Delta fT_sk}\mathrm{e}^{-\mathrm{j}\phi_k} = \mathrm{e}^{\mathrm{j}\theta} + n'(k), \quad 0 \leqslant k \leqslant L-1. \tag{7}$$

Assuming that the in-phase and quadrature components of $r'(k)$ are I and Q respectively, we have $I = \cos(\theta + \alpha_k)$ and $Q = \sin(\theta + \alpha_k)$, where α_k is the phase error introduced by additive Gaussian white noise.

When the SNR is high, α_k is very small and can be estimated as $\hat{\theta} = \arctan(Q/I)$.

When the SNR is low, only then are multiple estimates used to improve their accuracy. This is done as follows:

$$I' = \frac{1}{N}\sum_{k=1}^{N} I_k = \frac{1}{N}\sum_{k=1}^{N}\cos(\theta+\alpha_k), \tag{8}$$

$$Q' = \frac{1}{N}\sum_{k=1}^{N} Q_k = \frac{1}{N}\sum_{k=1}^{N}\sin(\theta+\alpha_k). \tag{9}$$

The final carrier phase estimates are

$$\hat{\theta} = \arctan\left(\frac{Q'}{I'}\right) = \arctan\left(\frac{\frac{1}{N}\sum\limits_{k=1}^{N}\sin(\theta+\alpha_k)}{\frac{1}{N}\sum\limits_{k=1}^{N}\cos(\theta+\alpha_k)}\right). \tag{10}$$

The estimate in (10) is the minimum unbiased estimate [15].

It provides the Cramer-Rao bound (CRB) for carrier phase estimation, $\mathrm{CRB}(\theta) = (2L_0 \times \mathrm{SNR})^{-1}$, where L_0 is the typical length of the preamble sequence used to estimate carrier phase offset. SNR is the SNR in [15].

Burst communication frames typically include a preamble header sequence used for aiding synchronization, with a typical length of several tens to several hun-

dreds of symbols, depending on the receiver's operating SNR threshold. To achieve fast carrier capture, researchers have proposed various data-assisted carrier parameter estimation algorithms based on the preamble header, such as LR (Luise and Reggiannini), LW (Lovell and Williamson), MM (Mengali and Morelli), Fitz, and others. Fig. 6 shows the frequency offset estimation variances for these four algorithms at different SNRs, revealing that, except for the LW algorithm, the other three algorithms exhibit performance close to the CRB at low SNRs [16].

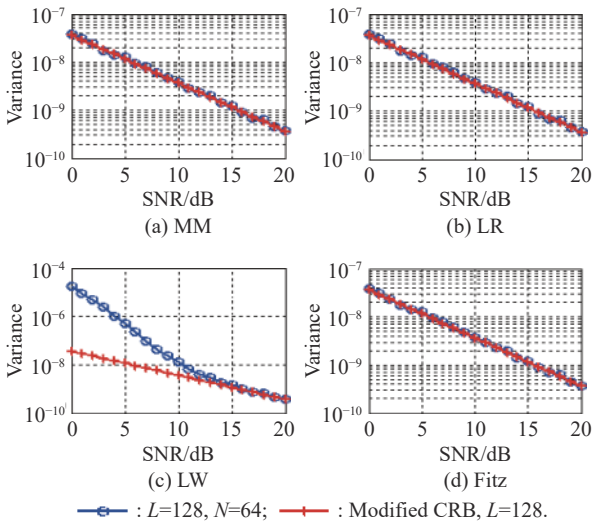

Fig. 6 Variance of frequency estimates at different SNR (with preambles length of 128)

However, at low SNR, such as 0 dB, the estimated normalized residual frequency offset after estimation for typical preambles with a length of 128 remains around 10^{-3}, as shown in Fig. 7. Therefore, the loop still requires a considerable number of symbols to successfully achieve synchronization.

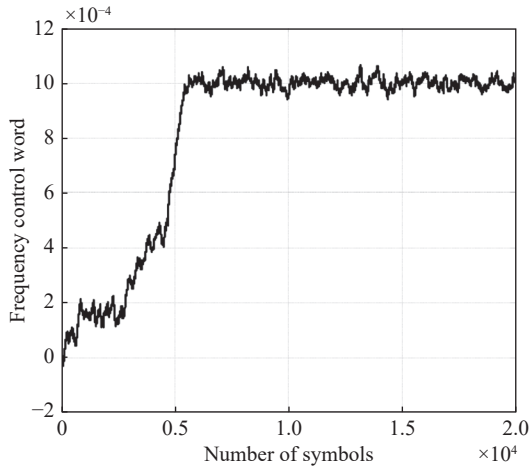

Fig. 7 Lock-in acquisition of the SNR at low SNR with a normalized residual frequency offset of 10^{-3}

According to the above simulation, it is known that open-loop algorithms can achieve fast reception of burst signals, but generally require a higher SNR threshold to operate. Under low SNR conditions, the estimation accuracy limitations lead to longer normal lock-in time with open-loop assistance. Existing algorithms are difficult to meet the requirements of low SNR and efficient burst communication.

It proposes a processing method for parameter estimation iterative demodulation in a true multi-high dynamic environment in [17], mainly aimed at improving performance in dynamic environments, with a simulated SNR of up to 3 dB. Pilot assisted methods are mainly used to achieve the estimation SNR of up to 0 dB in [18]. Its characteristic is that it requires a large amount of pilot and relatively low frame efficiency. It proposes a two-stage FFT correlation compensation method for short burst signals to improve their frequency and phase estimation accuracy, which requires a lot of resources and is not suitable for medium to high-speed signal processing in reference [19]. Convolutional neural network is proposed to improve the bit error performance under low SNR, which is characterized by high complexity and insufficient real-time performance in [20].

Unlike the above literature processing methods, this paper proposes a low SNR burst signal reception method suitable for onboard processing, called decode-assisted bidirectional variable-parameter iterative carrier synchronization technique.

3. Decode-assisted bidirectional variable-parameter iterative carrier synchronization technique

After conducting a thorough comparison of dozens of methods for tracking carriers, comprehensive performance results were obtained in the study presented in [21]. The results, as shown in Fig. 8, indicate that the different algorithms exhibit varying levels of adaptability in three common application scenarios which consist of smooth random influence, non-smooth random influence, and high dynamics. Overall, the closed-loop algorithm based on the PLL and its modified structure exhibits the best performance for smooth random influence, while the open-loop algorithm is more suitable for non-smooth random influence. The adaptive technique and the frequency-locked loop combined with the PLL show advantages in high dynamic conditions.

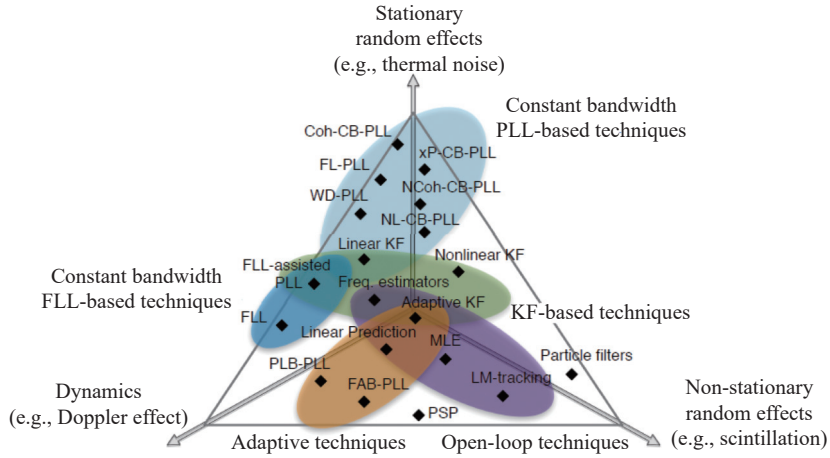

Fig. 8 Comprehensive performance comparison of carrier tracking algorithms

In HTS communication systems, the vast majority of applications are low-dynamic, and the satellite channel exhibits mainly Gaussian white noise characteristics. In such scenarios, closed-loop carrier tracking techniques such as PLL can achieve the best carrier tracking performance. This is the fundamental reason why PLL or similar techniques are commonly used in the DVB-S2 family of standard receivers.

The burst signal operating mode used in hopping beam technology is characterized by a short signal duration, which contradicts the long loop capture time of the PLL. This is the main reason why PLL technology is generally considered unsuitable for low SNR burst signal reception processing in burst signal receiver design. At present, it is generally accepted that open-loop carrier phase tracking technology should be used under such burst communication signal conditions. However, its performance under low SNR conditions cannot meet the system's usage requirements. This directly leads to a high SNR operating threshold of the hopping beam satellite receiver terminal, resulting in reduced forward and downward link performance of the HTS communication system. Ultimately, the total communication capacity of the entire system is reduced, and the expected effect of using hopping beam technology to improve the communication capacity of the system cannot be achieved.

At present, for broadband communication satellites, they generally operate in the Ka frequency band. Considering the stability and accuracy differences (usually in the 10^{-6} order) of satellite ground frequency sources, the frequency deviation generated in the Ka frequency band (taking 30 GHz as an example) can reach over 30 kHz. For medium to high-speed communication (taking 256 ksps symbol rate as an example), the relative deviation of this frequency deviation from the symbol rate can reach over 11.7%, making it impossible to use narrowband PLL tracking methods (generally less than 0.1%) for low signal ratio environments.

To address the aforementioned technical difficulties, this paper proposes a decode-assisted bi-directional variable-parameter iterative carrier synchronization technique. It can effectively improve the demodulation performance of burst signals with low SNRs, enabling the expected effect of using hopping beam technique to improve the communication capacity of the system to be realized.

3.1 Decode-assisted bidirectional variable-parameter iterative carrier synchronization algorithm architecture

In recent years, with the application of LDPC and other codes, scholars have proposed some decoding-assisted synchronization algorithms, which utilize the soft information output by the decoder to assist parameter synchronization in demodulation [22−24]. These algorithms can effectively estimate the carrier phase deviation at low SNR, but they all assume that the phase deviation is constant or can be considered constant within the encoding block, and can only work in the stable tracking phase, which cannot meet the above application requirements.

The bidirectional variable-parameter iterative carrier synchronization algorithm based on decoding assistance can reduce the requirement for the length of the preamble and can balance between the working threshold and algorithm complexity. This method adopts two technical measures in combination:

(i) Bidirectional variable-parameter iterative carrier synchronization;

(ii) Decoding-assisted judgment based on frequency partition presetting.

The architecture of the bidirectional variable-parameter iterative carrier synchronization algorithm based on

decoding assistance is shown in Fig. 9. It mainly includes an input buffer module, an initial frequency offset estimation module, a frequency offset partition presetting module, a bidirectional variable-parameter iterative carrier synchronization module, and a phase ambiguity resolution and soft-decision mapping module.

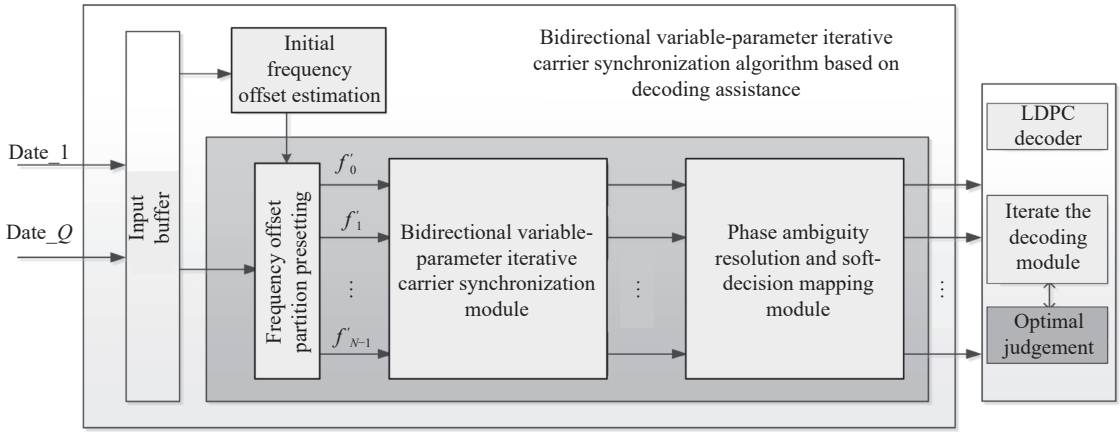

Fig. 9 Architecture of the bidirectional variable-parameter iterative carrier synchronization algorithm with decoding assistance

The architecture of the bidirectional variable-parameter iterative carrier synchronization algorithm includes several modules. The input buffer module stores the input information that has been synchronized by symbol synchronization. The initial frequency offset estimation module uses data-aided estimation algorithms (such as MM and LR) based on burst preamble to obtain the initial frequency offset f_c of the carrier. The frequency offset partition pre-setting module uniformly divides the residual frequency offset after initial frequency offset estimation into N sub-intervals according to its possible value range, with center frequency points $f'_0, f'_1 \cdots, f'_{N-1}$ in each sub-interval. The bidirectional variable-parameter iterative carrier synchronization module performs forward capture, iterative backtracking tracking, and forward tracking on the input information after frequency pre-setting using a second-order decision feedback loop. The phase ambiguity resolution and soft solution mapping module rotates the phase of the output information after carrier tracking based on the state of the unique word phase module, and outputs N-channel soft solution mapping information. The LDPC decoder performs channel decoding on the soft solution mapping information output by the modem. The optimal decision module is set in the decoder to select the optimal channel for decoding output from the N-channel soft solution mapping information.

3.2 Bidirectional variable-parameter iterative carrier synchronization

In coherent communication, PLL and their deformation structures are widely used. The loop design largely determines the performance of the communication system, and the commonly used second-order digital loop phase model is shown in Fig. 10.

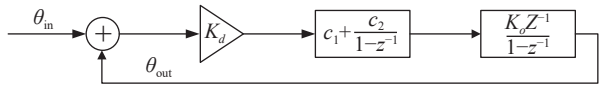

Fig. 10 Phase model of a second-order digital PLL

$K = K_d K_0$ is the loop gain and c_1, c_2 are the digital loop parameters. The equivalent phase noise caused by the input white noise, filtered by the loop, can be expressed as

$$\sigma^2_{\theta_{no}} = \left(\frac{S}{N}\right)^{-1}_i \frac{B_L}{B_i} \tag{11}$$

where B_i is the loop front-end filter bandwidth, $(S/N)_i$ is the ratio of the input signal power to the noise power passing through the front-end filter, and B_L is the loop noise bandwidth.

The ability of the loop to suppress noise can be reflected by the loop SNR, which is defined as

$$\left(\frac{S}{N}\right)_L = \frac{1}{\sigma^2_{\theta_{no}}} = \left(\frac{S}{N}\right)_i \frac{B_i}{B_L}. \tag{12}$$

Phase noise causes a deterioration of the BER and for a given target BER the corresponding loop S/N ratio can be calculated. In a real communication system, the input S/N ratio $(S/N)_i$ and the pre-filter bandwidth B_i are given. In order to keep the BER level at a low S/N ratio and to control the loop hopping probability, the loop bandwidth B_i must be narrowed. However, a smaller loop bandwidth B_i also means a longer capture-in time for the PLL, which creates a conflict between the fast synchronization and low SNR requirements mentioned earlier.

In this scenario, the PLL faces difficulties in meeting the requirements of burst signal demodulation due to its long capture-in-lock time. However, by drawing on the iterative process used in decoding, the input signal can be stored, and the previous loop run's frequency and phase estimation results can be used as a starting point for the iterative process. By iterating over the leading header data in both directions, the loop entry speed can be greatly accelerated. The reason for bi-directional iteration is that the frequency estimate and the direction of data processing are linearly related during the process of estimating carrier frequency bias. That is, the result of estimating from the beginning to the end of the data is opposite in sign to the inverse estimate. Therefore, to achieve continuous phase estimation of the signal, an inverse iteration operation is used. However, each time the direction is reversed, the sign of the current frequency bias estimate needs to be reversed as well. During the bi-directional iterative carrier synchronization process, the loop parameters can be continuously changed according to specific needs to adjust the intra-loop SNR and loop behavioral characteristics at different stages, thus achieving the best synchronization performance.

The processing flow of the algorithm is illustrated in detail in the following example. Fig. 11 shows a commonly used second-order loop.

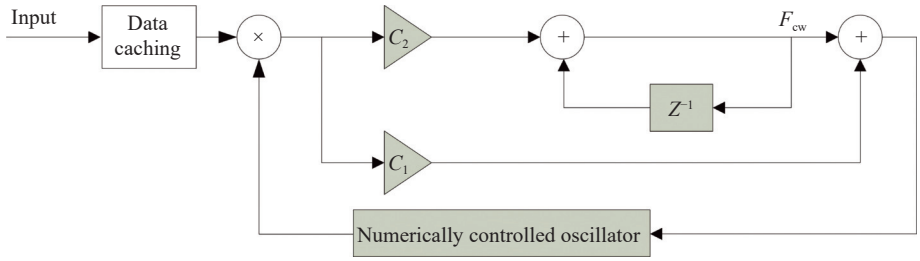

Fig. 11 Block diagram of a second-order digital PLL

When it uses the bidirectional variable-parameter iterative carrier synchronization algorithm, the processing of each burst data block is as follows.

Step 1 Estimate the initial frequency offset of the carrier using the leading header in the burst data block f_c and prepend it to the loop as the initial frequency control word $F_{cw}(0)$.

Step 2 Sequentially read out data Data(1) to Data(n) from the data cache, use the PLL for forward capture, monitor the loop in-lock situation in real time during the process, and decide the subsequent operation. If it is not locked after running to the end of Data(n), execute the subsequent Step 3; if it is locked, skip Step 3 and Step 4 to enter the tracking state.

Step 3 Invert the loop frequency control word, i.e., set to $-F_{cw}(N)$. Then, Data(n) to Data (1) are read out in reverse order from the data cache, and the PLL is used for reverse iterative synchronization. The lock-in condition of the loop is monitored in real-time during the process to determine the subsequent operation. If it is still not locked after running to the end of Data(1), proceed to Step 4; if it is locked, Step 4 can be skipped to enter the tracking state.

Step 4 The loop frequency control word is again inverted, i.e. set to $-F_{cw}(0)$. The data from Data (1) to Data(n) is read sequentially from the data cache, and the forward tracking is performed using a PLL. The loop is monitored in real time to determine the next operation. If the loop is not locked at the end of Data(n), Step 3 is performed; if it is locked, the trace state can be entered.

The maximum number of iterations is set during the bi-directional variable reference iterative carrier synchronization, and the algorithm process ends when the loop remains unlocked.

The process of the bi-directional parameterized iterative carrier synchronization algorithm is illustrated in Fig. 12. According to the requirements of a certain project, the simulation parameters are chosen as symbol rate of 2.4 Msps, initial frequency offset of 240 kHz, SNR of 0 dBm, binary phase shift keying (BPSK) modulation, 200 data bits for the preamble, and 1 000 bits for the simulated data. After using the bi-directional parameterized iterative carrier synchronization algorithm, the capture-in-lock curve of the loop is shown in Fig. 13. Fig. 13(a) shows the results of the algorithm running forward synchronization, reverse iterative synchronization, and forward iterative synchronization on the preamble data symbols in sequence. Fig. 13(b) shows the results of combining the bi-directional parameterized iterative process for comparison. From the results shown in Fig. 13, it can be seen that the new algorithm proposed in this paper can complete fast carrier locking by performing bi-directional parameterized iterative synchronization on 200 preamble data symbols, while traditional PLL methods require at least 600 symbols for locking. The bi-direc-

tional parameterized iterative carrier synchronization technique reduces the carrier synchronization time of burst signals to one-third of the original time, which fully meets the standard requirements of DVB-S2X.

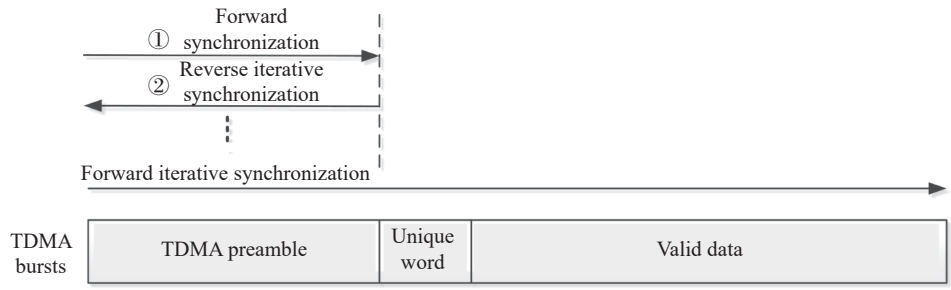

Fig. 12 Schematic diagram of bi-directional iterative carrier synchronization technique

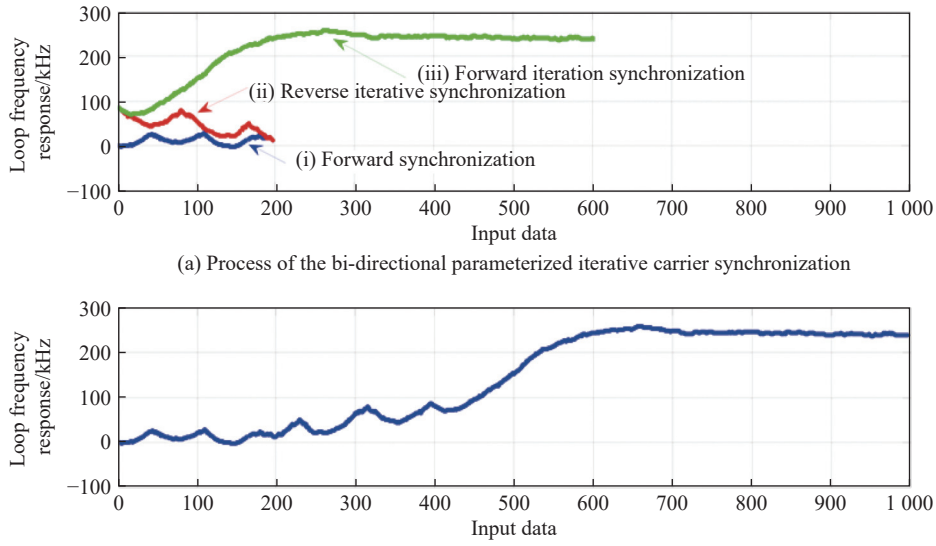

(a) Process of the bi-directional parameterized iterative carrier synchronization

(b) Process of the bi-directional parameterized iterative carrier synchronization (expand sequentially)

Fig. 13 Curve of bi-directional variable-parameter iterative carrier synchronization

3.3 Decoding-assisted judgement based on frequency partitioning presets

By utilizing bi-directional variable parameter iterative carrier synchronization technology, PLL can be applied to burst signal carrier synchronization. However, under low SNR conditions, if the residual frequency offset after carrier estimation is still relatively large compared to the loop bandwidth, forward capture of the PLL requires a long time to lock, which requires a large storage area for data buffering on the one hand, and also limits the application of bi-directional variable parameter iterative carrier synchronization technology in short burst communication on the other hand. Therefore, we propose a decoding-assisted decision-making technique based on frequency partition presetting.

In practical systems, the most commonly used decoding is the LDPC code. The LDPC code is a type of linear block codes that can be defined by very sparse parity-check matrices. When combined with the iterative decoding based on belief propagation (BP), it has the performance of approaching the Shannon limit. There are various decoding methods for LDPC codes, mostly based on message iterative decoding on factor graphs, and the most commonly used one is the BP algorithm. Due to its high hardware implementation complexity, simplified algorithms such as the minimum sum algorithm and its improved algorithms are often used in practical engineering applications. The messages transmitted during the LDPC iterative decoding process include channel initial message, check node message transmitted to variable node, variable node message transmitted to check node, and information collected by variables. When correctly decoded, the information collected by variables and presents a trend of continuous growth with the increase of

iterations.

Based on the characteristics of LDPC decoding, the signal amplitudes I and Q received without carrier frequency offset are the maximum, while in the presence of carrier frequency offset, the received signal needs to be multiplied by a phase offset term, which changes the effective amplitude relationship of the actual received signal and causes a corresponding decrease in likelihood ratio soft information. Through research, it is found that there is a correlation between carrier tracking and LDPC decoding output soft information. Specifically, the smaller the residual carrier frequency and phase deviation, the larger the sum of the absolute values of the decoding output soft information. Therefore, the sum of the absolute values of all codeword soft information can be accumulated as the objective function and used as the criterion for judging the quality of carrier synchronization.

Assume that the LDPC code check matrix is $\boldsymbol{H}$, the set of variable nodes i connected to the jth check node is $M(i)=\{j:H_{j,i}=1\}$, c_i, x_i and y_i, are the ith code element, the verdict signal and the received signal respectively, $L(c_i)$ is the log-likelihood ratio of the channel input information, r_{ji} is the probability of the external information passed from the check node i to the variable node j respectively, and Q_i is the probability of the soft information of the verdict variable node c_i. The coding-assisted judgement process based on frequency partitioning preconditioning is as follows:

(i) The carrier initial frequency offset f_c is estimated using the preamble header, and the possible distribution range of the residual frequency is set to $[-df_{\max}, df_{\max}]$. It is uniformly divided into N sub-intervals, and the center frequency point of each interval is $(\Delta f_1, \Delta f_2, \cdots, \Delta f_N)$. The initial frequency bias f_c is preset to obtain N fine frequency biases $(f_1, f_2, \cdots, f_N)$, where $f_i = f_c + \Delta f_i$ $(i \in [1,2,\cdots,N])$.

(ii) Based on each fine frequency offset, carrier synchronization and soft demapping are performed using the aforementioned bidirectional iterative carrier tracking, resulting in N demodulation results, which are then fed to the LDPC decoder.

(iii) Define the objective function

$$\psi(f_n)=\sum_{i=1}^{N}\left|L\left(Q_i^{(l)}\mid f_n\right)\right|= \sum_{i=1}^{N}\left|L(c_i\mid f_n)+\sum_{j\in M(i)}L(r_{ji}\mid f_n)\right| \tag{13}$$

where l denotes the number of iterations, f_n denotes the nth fine frequency bias, and $L\left(Q_i^{(l)}\mid f_n\right)$, $L(c_i\mid f_n)$ and $L(r_{ji}\mid f_n)$ denote the soft information of the variable node judgement, the input log-likelihood ratio and the external information obtained at that carrier frequency bias, respectively. When $\psi(f_n)$ is the maximum, the corresponding frequency bias is the optimal frequency bias

$$f_{\text{opt}}=\arg\max_{n\in[1,N]}\left[\psi(f_n)\right]. \tag{14}$$

Its corresponding demodulation result is least affected by frequency bias and has the highest accuracy, and is decoded as the final output.

Fig. 14 shows the variation of the objective function $\psi(f_n)$ with the iteration number for the optimal frequency offset preset and non-optimal frequency offset preset. In the simulation, the quantization of the soft information before decoding is performed using 6-bit signed numbers, i.e., a numerical range of [−32, 31]. When the preset frequency is the optimal frequency offset, the value of the objective function $\psi(f_n)$ increases rapidly with the increase of the iteration number, and after three iterations, the value of the objective function exceeds 5 000. When the preset frequency is non-optimal, the value of the objective function $\psi(f_n)$ does not increase with the increase of the iteration number and is much lower than 5 000.

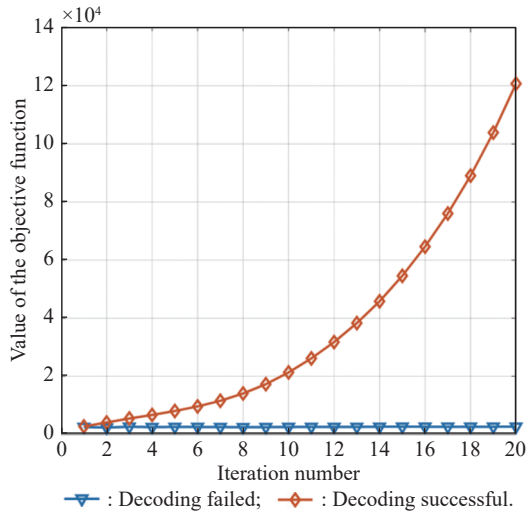

Fig. 14 Trend of the change of the target function metric with iteration number

The number of frequency offset partitions needs to be carefully considered, as increasing the number of partitions can reduce the deviation of a fine frequency offset from the true frequency offset, resulting in more accurate demodulation results. However, this also means an increase in the implementation complexity of carrier synchronization, demapping, and decoding. In practical applications, a comprehensive consideration of perfor-

mance requirements and processing resources is necessary. Simulation results are shown in Fig. 15.

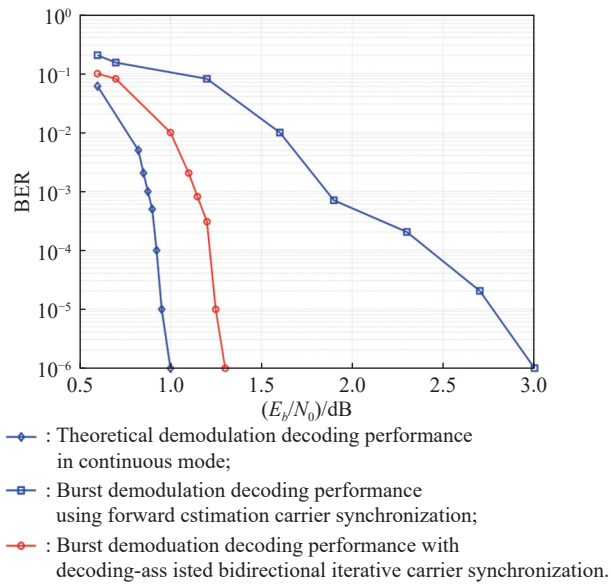

Fig. 15 Performance comparison of the bidirectional iterative carrier synchronization technique with decoding assistance

According to the simulation results, it can be seen that the burst demodulation performance using the proposed decoding-assisted bidirectional iterative carrier synchronization technique is better than that using the forward estimation carrier synchronization technique and is close to the theoretical demodulation and decoding performance under continuous mode. When the BER is in the order of 10^{-6}, the degradation of burst demodulation performance achieved with this method is less than 0.3 dB compared to the theoretical demodulation and decoding performance under continuous mode.

3.4 Algorithm complexity analysis

The use of decoding-assisted bidirectional variable parameter iterative carrier synchronization technology essentially does not increase processing resources, and the main cost is to reduce the throughput of the entire reception processing under a certain working clock. The processing complexity will be analyzed from the perspective of time cost below.

Assuming the symbol length of the received signal is W, the symbol length using iterative tracking processing is M, the number of frequency presets is N, the number of complete decoding iterations is U, and the number of iterations to remove abnormal data is V, then the consumption of the received carrier synchronization under the traditional PLL method is W, and the iteration consumption is U. For the carrier synchronization implementation using decoding assisted bidirectional variable parameter iterative carrier synchronization technology, the consumption is $(2M+W)N$, and the iteration number consumption is $V(N-1)+U$.

For broadband signals, the frequency deviation relative to the symbol rate will be greatly reduced, and the frequency preset quantity parameter N will also be reduced, which to some extent weakens the impact. In broadband signals where the relative frequency offset is still relatively high, parallel processing algorithms need to be used to improve performance by increasing resources.

4. Conclusions

This paper begins by analyzing the key issues in burst communication of service signals in the hopping beam system. Based on this analysis, a comparative study of typical algorithms for carrier synchronization of burst signals is conducted. Next, a decode-assisted bidirectional variable-parameter iterative carrier synchronization technique is proposed, which combines the need for efficient burst and low SNR reception of forward link downlink signals in the hopping beam communication system. The paper introduces the idea of iterative processing into carrier synchronization and adopts a new technical approach of bi-directional variable-parameter iterative carrier synchronization that breaks through the traditional understanding that the loop structure cannot adapt to low SNR burst demodulation. Finally, the paper conducts a study and performance simulation in conjunction with the DVB-S2X standard physical layer frame format used in HTS communication systems. The results show that the proposed new technique can significantly reduce the carrier synchronization time of burst signals and achieve fast synchronization of low SNR burst signals. It also has the unique advantage of flexible and adjustable parameters.

References

[1] ETSI EN 302 307-2 V1.2. 1. Digital video broadcasting (DVB); second generation framing structure, channel coding and modulation systems for broadcasting, interactive services, news gathering and other broadband satellite applications; part 2: DVB-S2 extensions (DVB-S2X). Berlin: German Society for Standardization, 2020.

[2] GONG X F. Research on burst demodulation technology of low signal-to-noise ratio QPSK in satellite communication. Beijing: China Academy of Space Technology, 2011. (in Chinese)

[3] EURP L, GARDNER F M. Interpolation in digital modems—part II: implementation and performance. IEEE Trans. on Communications, 1993, 41(6): 502–508.

[4] LIU C L. Research and implementation of efficient coding modulation scheme based on LDPC codes. Beijing: Beijing

Institute of Technology, 2008. (in Chinese)
[5] CASINI E, GAUDENZI R D. DVB-S2 modem algorithms design and performance over typical satellite channels. International Journal of Satellite Communications and Networking, 2004, 22: 281–318.
[6] MENGALI U. Synchronization techniques for digital receivers. New York: Plenum Press, 1997.
[7] FITZ M P, CRAMER J M. A performance analysis of a digital PLL based MPSK demodulator. IEEE Trans. on Communications, 1995, 43: 1192–1201.
[8] KAY S. A fast and accurate single frequency estimator. IEEE Trans. on Acoustics Speech and Signal Processing, 1989, 37(12): 1987–1990.
[9] FTIZ M. Planar filtered techniques for burst mode carrier synchronization. Proc. of the IEEE Telecommunications Conference, 1991: 365−369.
[10] LUISE M, REGGINANINI R. Carrier frequecy recovery in all-digital modems for burst-mode transmissions. IEEE Trans. on Communications, 1995, 43: 1169–1178.
[11] MENGALI U, MORELLI M. Data-aided frequency estimation for burst digital transmission. IEEE Trans. on Communications, 1997, 45(1): 23–25.
[12] RIFE D C, BOORSTYN R. Single-tone parameter estimation from discrete-time observation. IEEE Trans. on Information Theory, 1974, 20(5): 591–598.
[13] CALVO P M, SEVILLANO J F, VELEZ I. Enhanced implementation of blind carrier frequency estimators for QPSK satellite receivers at low SNR. IEEE Trans. on Consumer Electronics, 2005, 51(2): 442–448.
[14] GONG C, ZHANG B N, GUO D S. A quick and accurate union carrier parameter estimation algorithm based on FFT. Acta Electronica Sinica, 2010, 38(4): 766–770.
[15] VITERBI A J, VITERBI A M. Nonlinear estimation of PSK modulated carrier phase with application to burst digital transmission. IEEE Trans. on Information Theory, 1983, 29(4): 543–551.
[16] ANDREA A, MENGALI U, REGGIANNINI R. The modified Cramer-Rao bound and its application to synchronization problems. IEEE Trans. on Communications, 1994, 42(234): 1391–1399.
[17] LIU Y , ZHOU X X, CHENG G. High dynamic carrier tracking technology in frequency hopping systems. Systems Engineering and Electronics, 2022, 44(2): 677–683. (in Chinese)
[18] LI S Y. Research of high efficient receiver synchronization techniques in burst communication systems. Xi'an: Xidian University, 2018. (in Chinese)
[19] WANG C H, GAO F. A coherent demodulation method for short burst communication systems. Proc. of the IEEE 8th Joint International Information Technology and Artificial Intelligence Conference, 2019. DOI: 10.1109/ITAIC.2019.8785516.
[20] QIANG Z K, YAN T F. Demodulation of low SNR QPSK signal based on CNN. Proc. of the International Conference on Intelligent Transportation, Big Data and Smart City, 2021. DOI: 10.1109/ICITBS53129.2021.00162.
[21] LOPEZ S. Survey on robust carrier tracking techniques. IEEE Communications Surveys & Tutorials, 2014, 16(2): 670–688.
[22] SKONG I, HANDEL P. Synchronization by two-way message exchanges: Cramer-Rao bounds approximate maximum likelihood and offshore submarine positioning. IEEE Trans. on Signal Processing, 2010, 58(4): 2351–2362.
[23] ZHANG Q, YU Z Y, BAI B M . Carrier synchronizator in nonbinary LDPC coded modulation systems. Proc. of the International Conference on Communications and Networking, 2017. DOI: 10.1007/978-3-319-78139-6_13.
[24] VALLES E L, RICHARD D W, JOHN D V, et al. Pilotless carrier phase-synchronization via LDPC code feedback. Proc. of the Military Communications Conference, 2010. DOI: 10.1109/MILCOM. 2010.5680463.

Biographies

ZHAI Shenghua was born in 1978. He received his M.S. degree from Harbin Engineering University, Harbin, China, in 2004 and his D.Eng. degree from Beijing Institute of Technology in 2021. He is currently a principal investigator in China Academy of Space Technology and a professor in CAST (China Academy of Space Technology)-Xi'an Institute of Space Radio Technology. His research interests include wireless communications, satellite communication systems, and digital signal processing.
E-mail: zhaish504@163.com

HUI Tengfei was born in 1983. He received his B.S degree from Xidian University, China, in 2005, and M.S. degree from China Academy of Space Technology (CAST), Beijing, China, in 2008. He is now a senior engineer at the Xi'an Branch of CAST. His research interests include satellite communication system design and communication signal processing.
E-mail: cast_huitf@163.com

GONG Xianfeng was born in 1982. He received his B.S. degree from Chongqing University of Posts and Telecommunications, China, in 2004, and M.S. degree from China Academy of Space Technology (CAST), Beijing, China, in 2011. He is now a senior engineer at the Xi'an Branch of CAST. His research interests include satellite communication system design and communication signal processing.
E-mail: gongxf1982@163.com

ZHANG Zehui was born in 1995. He received his B.E. degree in electronic information engineering from Chongqing University and is currently working towards his Ph.D. degree at the School of Cyberspace Security, Beijing Institute of Technology, Beijing, China. His research interests include wireless communication, wireless signal identification, artificial intelligence, cognitive radio, electronic warfare, and machine learning in communication.
E-mail: zzhui@bit.edu.cn

GAO Xiaozheng was born in 1992. He received his B.S. degree and Ph.D. degree from Beijing Institute of Technology, Beijing, China, in 2014 and 2020, respectively. He was a visiting student with the School of Computer Science and Engineering, Nanyang Technological University, Singapore. He is currently an associate professor in Beijing Institute of Technology. His current research interests include cellular communications, backscatter communications, and Internet of Things.
E-mail: gaoxiaozheng@bit.edu.cn

YANG Kai was born in 1983. He received his B.E. degree in communications engineering from National University of Defense Technology, Changsha, China, in 2005 and Ph.D. degree in communications engineering from Beijing Institute of Technology, Beijing, China, in 2010. He is currently a full professor with the School of Information and Electronics, Beijing Institute of Technology. His current research interests include convex optimization, massive multi-input multi-output, mmWave systems, resource allocation, and interference mitigation.
E-mail: yangkai@bit.edu.cn